# COMPUTER MODELING OF FLOW PATTERNS OBTAINED BY SCHLIEREN AND SHADOW TECHNIQUES

*J.Blažek* [1], *P.Kříž* [1], *J.Olejníček* [2], *P.Špatenka* [1]

[1] University of South Bohemia, Department of Physics, Jeronýmova 10, České Budějovice, Czech Republic

[2] Institute of Physics, Academy of Science, Na Slovance 2, Praha, Czech Republic

## 1. Introduction

There are three basic optical methods visualizing inner conditions in transparent objects like gas stream or low-temperature plasma: shadow, schlieren and interefometric techniques. All these three instruments are based on the dependence of the refractive index on the mass density varying in investigated space. In spite of common characteristics each instrument serves a different function.

The interferometric method is based on the phase shift obtained by the beam passing through the gas or plasma object. The phase shift depends directly on the refractive index or density and the method is therefore suitable for quantitative analysis. On the other hand, the interferogram is not appropriate for qualitative visualization, e.g. of shock waves or stagnation points. Moreover, the (holographic) interferometry is experimentally complicated and rather delicate.

Contrary to interferograms the schlieren and shadow images are very suitable for simple and understandable visualization of inner processes in flowing gas or cold plasma, but quantitative interpretation is almost impossible: The schlieren effect is caused by the refractive or density gradient, the shadowgraph even depends on the second derivatives of the refractive index. As a first step in attempt to estimate some gas or plasma parameters related to the refractive index, like density, pressure or temperature, we developed a MATLAB code which for inner conditions given in advance models the corresponding images. This program enables to interpret various image patterns, e.g. for gas flowing from one or several nozzles, gas impacting on the plane obstacle and so on.

## 2. Basic principles of schlieren and shadow techniques

Both these methods are based on refraction [1,2]. As they do not need any components introduced into investigated transparent medium, they can be used to study press or temperature fields without disturbing or influencing the medium.

If the index of refraction is close to unity, as it is for gases, the empirical Gladstone-Dale equation connecting the refractive index with mass density $\rho$ approximately holds:

$$\frac{n-1}{\rho} = K \qquad (1)$$

where constant $K$ depends on chemical composition and wavelength of the light. This equation may be expressed equivalently

$$n = n_0 + (n_0 - 1)\left(\frac{\rho}{\rho_0} - 1\right) \qquad (2)$$

where quantities with zero subscript are related to the homogeneous reference state. For perfect gas it reads

$$n = n_0 + (n_0 - 1)\left(\frac{T_0}{p_0}\frac{p}{T} - 1\right) \tag{3}$$

where $p$ and $T$ are pressure and temperature, respectively.

**Schlieren system**

As a light source is commonly used mercury lamp. In our arrangement we have also equipped the system with a laser source. In front of the chamber is a lens 4 (Fig.1) forming a parallel beam. Another lens 6 placed behind the chamber focuses the image of the light source on its focal plane. In the image position is placed a knife-edge 8 partly overlapping the image of the light source 3 and by that way controlling the light intensity. Other optical elements display this overlapped image on the screen or – as in our case – on an objective of CCD camera.

The beam passing through the medium – gas or plasma – undergoes a small deflection depending upon the gradient of the refractive index. As a result, the image in the focus plane is shifted above or below the knife-edge and the intensity of the screen illumination is changed proportionally to the shift. To express the change of illumination quantitatively, let us orient the Cartesian coordinates so that the *x*-axis is pointed to the direction of light propagation and *z*-axis is oriented perpendicularly to the knife-edge. Then the deflection in the *z*-direction is [1]

$$z' \approx \frac{1}{n_0}\int_{x1}^{x2} \frac{\partial n(x, y_1, z_1)}{\partial z}\,\mathrm{d}x \tag{4}$$

or, substituting Eq. 2,

$$z' \approx (n_0 - 1)\int_{x1}^{x2} \frac{\partial \sigma(x, y_1, z_1)}{\partial z}\,\mathrm{d}x, \qquad \sigma \equiv \frac{\rho - \rho_0}{\rho_0}. \tag{5}$$

The changes of the position at the plane perpendicular to the *x*-axis are neglected, therefore the light beam entries the chamber in the point $(x_1, y_1, z_1)$ and exits it in the point $(x_2, y_1, z_1)$. Analogous formula holds for deflection $y'$ in the *y*-direction.

Now let us suppose the image of the source made by the lens 6 of the focal length $f$ is a rectangular of the width *w* parallel to the *y*-axis ("horizontal" side) and height *h* parallel to the *z*-axis ("vertical" side). Let the knife-edge is parallel to the side *w* and for undisturbed case shields a part *h-a* of the image height so that the area *w*×*a* of the image above the knife edge causes illumination $I$ of the screen. The deflection $z'$ of the light beam displaces the image a distance $\Delta z = f\, z'$ from its original position of the knife-edge. This shift changes the intensity $I'$ on the screen,

$$\frac{I'}{I} = \frac{a'}{a} \tag{6}$$

where

$$a' = \begin{cases} a - \Delta z, & -(h-a) < \Delta z < a \\ 0, & \Delta z > a \quad \text{(whole image hidden by the knife)} \\ h, & \Delta z < -(h-a) \quad \text{(whole image above the knife-edge)} \end{cases} \tag{7}$$

The deflections are usually so small that only the first expression for $a'$ in Eq. 7 comes into question. Tiny shifts of the image above or below the diaphragm edge cause observable changes in the illumination on the screen. From the relative change of the illumination one can determine the deflection in the direction perpendicular to the edge.

In the above equations we have supposed the knife edge is parallel to the *y*-axis. If the whole measuring system (except the chamber) is turned by the angle $\alpha$ about *x*-axis then the deflection perpendicular to the knife-edge is $z'\cos\alpha + y'\sin\alpha$ .

**Shadowgraph system**

As the schlieren effect is caused by the first derivatives of the density, the schlieren system is used most advantageously when the density gradient varies gradually. If the density varies rapidly, the shadow technique depending on the second derivatives is more useful.

The experimental arrangement for shadowgraph technique is much simpler than for the schlieren method as it does not use the knife-edge. It is based on the fact that the beam of originally parallel rays becomes in inhomogeneous medium convergent or divergent. This phenomenon is manifested as a brighter or darker light spot on the projection screen compared with the parallel beam. It can be shown that for shadowgraph [1]

$$I' = \frac{I}{1 + \dfrac{L}{n_0} \displaystyle\int_{x1}^{x2} \left[ \frac{\partial^2 n}{\partial y^2} + \frac{\partial^2 n}{\partial z^2} \right] \mathrm{d}x} \tag{8}$$

where $L$ is the distance of the screen from the chamber. The axes are oriented as before, i.e. the *x*-axis is oriented in the direction of the light propagation.

## 3. Experimental setup

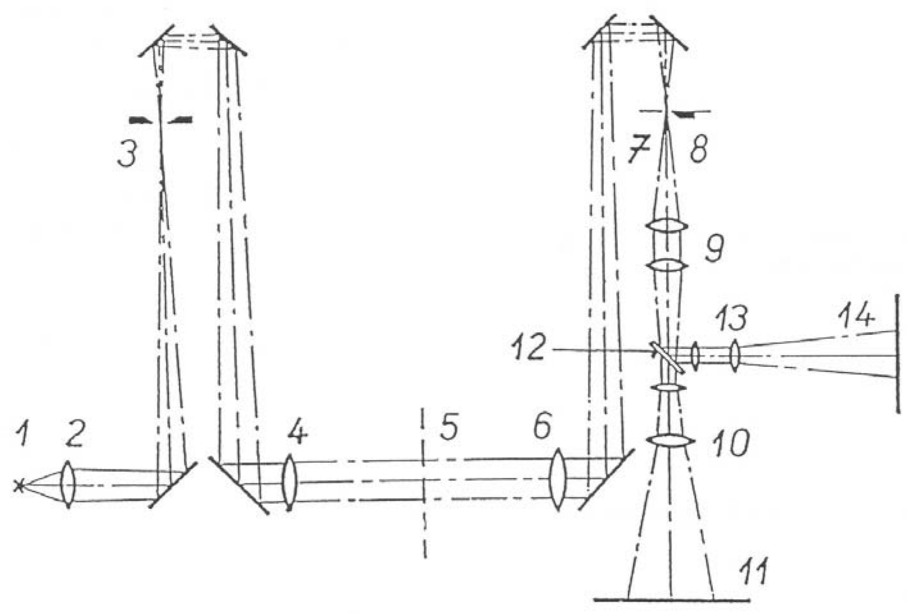


**Fig. 1** Schlieren equipment made by Carl Zeiss Jena.

The set up of the schlieren equipment made by Carl Zeiss Jena is depicted in Fig. 1. Either He-Ne laser or high pressure mercury vapour lamp is used as a light source 1. The light beam goes through the condenser 2 and slit 3 placed in the focus of the first main lens 4. Then it passes through the observed area 5 and the second main lens of the system, 6. In its focus is placed a schlieren element 8 (knife-edge or grid). The lenses 9 and 10 project the observed object into the classical or CCD camera 11.The inclinable mirror 12 enables to reflex the light beam through the object lenses 13 to the screen 14 in case of visual observations. With the described equipment it is possible to realize classical as well as colour schlieren method. Without the schlieren element 8 this equipment can be adjusted to the shadowgraph technique.

The images need some computer-aided processing like noise filtering or contrast increasing. Fig. 2 shows complex setup of the equipment including connection with a computer.

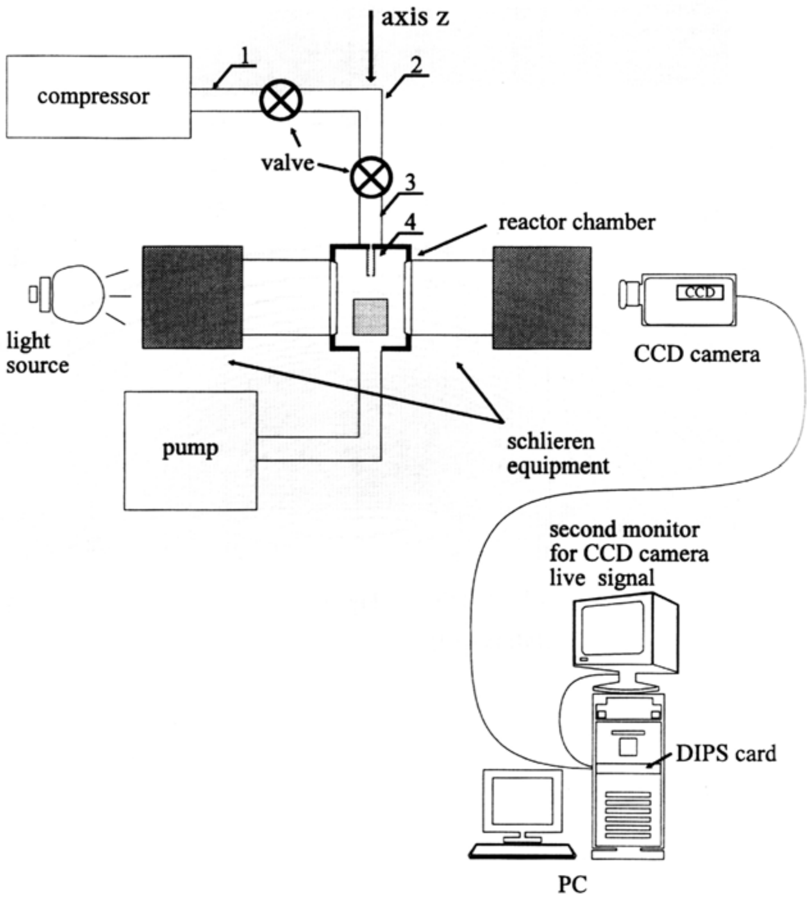


**Fig. 2** General arrangement of experiment

## 4. Numerical modeling of schlieren and shadow images

In the MATLAB environment we have developed codes, which for given distribution of temperature, pressure or density theoretically reconstruct corresponding images obtained by schlieren or shadow technique. The computations were made for air, which for normal pressure $p_0 = 1.013\times10^5$ Pa, temperature $T_0 = 293.15$ K and wavelength $\lambda = 632.8$ nm (laser source of light) has the refractive index $n_0 = 1.0002716$.

Both codes have similar structure. For given process (gas flow, plasma discharge) a relative change of density $\sigma$ is defined as a function of coordinates. Its first (schlieren method) or second (shadowgraph) derivatives are expressed either analytically, or – if analytical expressions are too complicated or cumbersome – numerically. In the second case the data is first interpolated by cubic spline (MATLAB function spline) and then the piecewise polynomial is differentiated analytically (MATLAB function fnder). If the derived function $\sigma$ is numerically overlapped by noise, the least-squares spline approximation (MATLAB function spap2) is applied instead of spline interpolation.

So far we have tested axially symmetric functions of the general form

$$\sigma(r,z) = A(z)\cdot \exp[-B(r,z)] \tag{9}$$

where $z$-coordinate is oriented along symmetry axis and $r = \sqrt{x^2 + y^2}$ is radial coordinate. Functions $A$, $B$ are expressed through elementary functions like polynomials or exponentials.

Fig. 3 shows an example of such modeling for functions

$$A(z) = C\cdot\left[1 - \frac{z}{L}\exp\left(1 - \frac{z}{L}\right)\right], \qquad\qquad B(r) = D\cdot\left(\frac{r}{R}\right)^2 \tag{10}$$

where $L$ is the length of a cylindrical chamber, $R$ is its radius and $C$, $D$ are scaling constants.

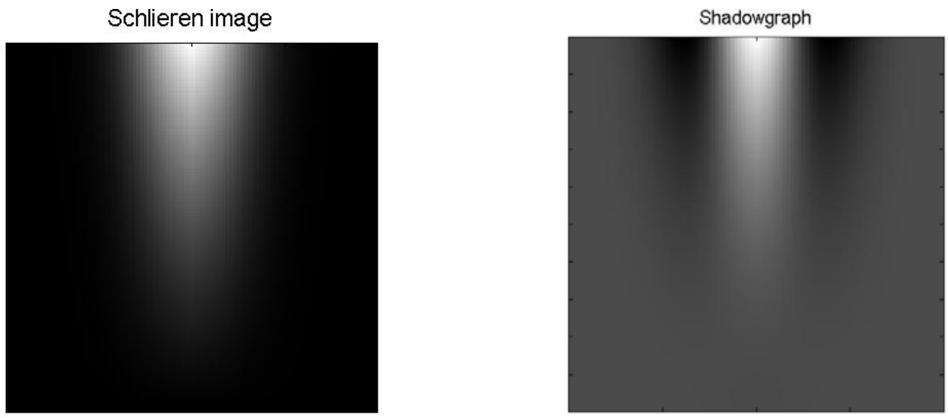


**Fig. 3** Examples of computer modeling of images obtained by refractional techniques

## 5. Conclusion

In this paper we have solved how to reconstruct a refractive image for given distribution of mass density (temperature – pressure), but much more important is the solution of the inverse problem – how to find the density distribution from the image of real process. As the refractive methods depend on the first (Eq. 5) or second (Eq. 8) derivatives, they are not as suitable for this purpose as are interference methods [4,5]. Nevertheless, some possibilities to obtain quantitative estimations from refractive methods exist. For instance, we can compare images modeled for densities theoretically predicted by gas dynamics (e.g. [3]) with the real ones. We can also employ empirical formulas, such as Eqs. 9,10, with optional parameters specified by the least squares method based on comparison of model and real image. Last but not least there is a possibility to apply inverse integral transformations to Eqs. 5,8. As is known, for axially symmetric integrands there exists inverse Abel transformation [5,6]. This transformation cannot be directly applied to refractive methods as the axial symmetry of mass density (see Eq. 9) is violated by the differentiation with respect to $y$. Fortunately, as the dependence of the integrand upon variable $y$ is known, one can derived the inverse transformation analogously to the method [5], when the axially symmetric object is divided into discrete system of annular elements and the integral transformation is replaced by the system of linear equations. Analysis of the inverse problem will be subject of our next article.

**Acknowledgment**

This work has been supported by the grant 202/05/2242 from the Grant Agency of the Czech Republic.

**References**

[1] R. Řezníček: Visualizace prodění. Academia, Praha 1972.

[2] W. Merzkirch: Flow Visualization. Academic Press, London 1970.

[3] G.K. Batchelor: An introduction to Fluid Dynamics. Cambridge University Press, 1967.

[4] J. Blažek, P. Kříž, V. Stach, Czech. J. Phys. 50/S3 (2000), 397.

[5] C.M. Vest: Holographic Interferometry. John Wiley & Sons, New York 1979.

[6] R. Bracewell: The Fourier Transform and its Applications. New York 1965.

**Contact:**

Josef Blažek
Department of Physics, University of South Bohemia
Jeronýmova 10, 371 15 České Budějovice
Czech Republic
E-mail: bla@pf.jcu.cz